Available online at www.sciencedirect.com
SCIENCE DIRECT®
Journal of Sound and Vibration 288 (2005) 1223–1239
JOURNAL OF SOUND AND VIBRATION
www.elsevier.com/locate/jsvi

Improvement of impulse response spectrum and its application

Se Jin Ahn[a,1], Weui Bong Jeong[b,*], Wan Suk Yoo[b]

[a]*Research Institute of Mechanical Technology, Pusan National University, Busan, Republic of Korea*
[b]*School of Mechanical Engineering, Pusan National University, Busan, Republic of Korea*

Received 28 November 2003; received in revised form 24 November 2004; accepted 28 January 2005
Available online 15 April 2005

Abstract

Since the impulse response of a system is a transient and non-stationary signal, difference of record length makes the unit impulse response spectrum of the system to be not unique. It means that the magnitudes and phases of the frequency response function obtained from impact hammer testing depend on the record length. Whenever the record length is not longer than the duration time during which the impulse response completely diminishes, 'finite record length error' takes place in the impulse response spectrum. In this paper, the finite record length error is theoretically verified and a new method reducing the error is introduced. The system parameters to induce the finite record length error are investigated, and an optimization method is also proposed to reduce this error. Numerical and experimental examples are carried out to show the characteristics of the finite record length error and the validity of the new method proposed in this paper.

1. Introduction

Impact hammer testing has been used in wide area of engineering to get frequency response function (FRF) owing to its convenience and simplicity on experimentation as well as its validity on analysis procedure [1–3]. There have been various works in which some kinds of problem such

*Corresponding author. Tel.: +82 51 510 2337; fax: +82 51 517 3805.
E-mail address: wbjeong@pusan.ac.kr (W.B. Jeong).
[1]Currently at: Institute of Sound and Vibration Research, University of Southampton, Southampton, UK.

0022-460X/$ - see front matter © 2005 Elsevier Ltd. All rights reserved.
doi:10.1016/j.jsv.2005.01.020

as leakage error, the ratio of signal to noise (S/N ratio), low-pass filtering, nonlinearity, window function and so on are improved to get more accurate FRF from impact hammer testing [4–6].

When a system is excited by an impact hammer, the system vibrates for a while and the response finally dies down. In fact, the time duration of the free vibration depends on the physical characteristics of the system, especially its damping coefficient. The record length for signal analysis is usually restricted by the memory size and computation time of the dynamic analyzer. It is difficult to have a record length longer than the time duration of the signal for system having low damping coefficient. In this case, significant errors occur in the FRF obtained by impact hammer testing [7,8]. It is termed as finite record length error in this paper.

In this paper, the finite record length error in a FRF is theoretically identified by using the unit impulse response function. The disadvantage of applying an exponential window function to an impulse response signal is also proved analytically [9]. After the correct expression for the impulse response spectrum considering the finite record length error is derived, a new method is suggested to estimate the modal parameters of the system by using the expression. Numerical and experimental examples are carried out to show the validity and usefulness of the new method proposed in this paper.

2. Theoretical background

2.1. Finite record-length error in impulse response spectrum

The equation of motion of a viscously damped 1-dof system is described as follows

$$m\ddot{x}(t) + c\dot{x}(t) + kx(t) = f(t). \tag{1}$$

The impulse response under unit impulse input of the Dirac delta function is well known as

$$h(t) = \frac{e^{-\zeta\omega_n t}}{m\omega_d}\sin\omega_d t, \quad t \geqslant 0, \tag{2}$$

where $h(t)$, ζ, and ω_d mean unit impulse response function, damping ratio, and damped angular frequency of a system, respectively. Considering a field test such as impact hammer testing, the infinite time cannot be integrated and must be modified for a record length T_{RL} when Fourier transformation is carried out. And then the Fourier transformation of $h(t)$ in Eq. (2) is written as

$$H(\omega)\big|_{T_{RL}} = \int_0^{T_{RL}} \frac{e^{-\zeta\omega_n t}}{m\omega_d}\sin\omega_d t e^{-j\omega t}\,dt = \frac{1}{k-\omega^2 m + j\omega c}[1 - E(\omega)|_{T_{RL}}], \tag{3}$$

where

$$E(\omega)\big|_{T_{RL}} = e^{-\zeta\omega_n T_{RL}} e^{j\omega T_{RL}}\left\{\frac{\zeta}{\sqrt{1-\zeta^2}}\sin\omega_d T_{RL} + \cos\omega_d T_{RL} + j\frac{\omega}{\omega_d}\sin\omega_d T_{RL}\right\} \tag{4}$$

represents the finite record length error in this paper, and T_{RL} is the record length during which the signal is acquired in an impact hammer testing. If the record length T_{RL} were infinite, the finite

record-length error could disappear and then the FRF be

$$H(\omega) = \lim_{T_{\mathrm{RL}}\to\infty} H(\omega)\big|_{T_{\mathrm{RL}}} = \frac{1}{k-\omega^2 m + \mathrm{j}\omega c} = \frac{1/k}{1-(\omega/\omega_n)^2 + \mathrm{j}2\zeta(\omega/\omega_n)}. \tag{5}$$

This means that the FRF obtained from an impact hammer testing would match the theoretical FRF only when the record length is infinite. However, the finite record length error is not actually avoidable because the record length should be inevitably finite in the real test condition such as impact hammer testing.

2.2. Distortion of FRF caused by exponential window function

Exponential window function is usually applied to an impulse response signal in order to reduce the finite record length error as well as the leakage error which takes place when the record length is not sufficiently long. If an exponential window function with decay rate α is applied to Eq. (2), the unit impulse response is revised as

$$h_w(t) = \mathrm{e}^{-\alpha t}\frac{\mathrm{e}^{-\zeta\omega_n t}}{m\omega_d}\sin\omega_d t, \quad t \geqslant 0. \tag{6}$$

When the time data is acquired for a record length T_{RL}, the Fourier transformation of Eq. (6) is described as [9,10]

$$\begin{aligned}\bar{H}_w(\omega)|_{T_{\mathrm{RL}}} &= \int_0^{T_{\mathrm{RL}}} \mathrm{e}^{-\alpha t}\frac{\mathrm{e}^{-\zeta\omega_n t}}{m\omega_d}\sin\omega_d t\,\mathrm{e}^{-\mathrm{j}\omega t}\,\mathrm{d}t \\ &= \frac{1/k}{1-(\omega/\omega_n)^2 + 2\zeta(\alpha/\omega_n) + (\alpha/\omega_n)^2 + \mathrm{j}2(\zeta+\alpha/\omega_n)\omega/\omega_n}[1 - E_w(\omega)|_{T_{\mathrm{RL}}}],\end{aligned} \tag{7}$$

where

$$\begin{aligned}E_w(\omega)\big|_{T_{\mathrm{RL}}} = \mathrm{e}^{-(\alpha/\omega_n+\zeta)\omega_n T_{\mathrm{RL}}}\Bigg[&\frac{\omega}{\omega_d}\sin\omega_d T_{\mathrm{RL}}\sin\omega T_{\mathrm{RL}} + \left(\frac{\alpha}{\omega_n}+\zeta\right)\frac{\omega_n}{\omega_d}\sin\omega_d T_{\mathrm{RL}}\cos\omega T_{\mathrm{RL}} \\ &+ \cos\omega_d T_{\mathrm{RL}}\cos\omega T_{\mathrm{RL}} + \mathrm{j}\Bigg\{\frac{\omega}{\omega_d}\sin\omega_d T_{\mathrm{RL}}\cos\omega T_{\mathrm{RL}} \\ &- \left(\frac{\alpha}{\omega_n}+\zeta\right)\frac{\omega_n}{\omega_d}\sin\omega_d T_{\mathrm{RL}}\times\sin\omega T_{\mathrm{RL}} - \cos\omega_d T_{\mathrm{RL}}\sin\omega T_{\mathrm{RL}}\Bigg\}\Bigg].\end{aligned} \tag{8}$$

The $E_w(\omega)\big|T_{\mathrm{RL}}$ given in Eq. (8) represents the finite record length error of the exponentially windowed FRF. It is known from Eq. (8) that the finite record length error still remains in the FRF if the decay rate α or the record length T_{RL} is finite. By selecting a large decay rate of the exponential window function, the finite record length error $E_w(\omega)$ can be removed so that the fully windowed FRF becomes

$$\check{H}_w(\omega)\big|_{T_{\mathrm{RL}}} = \frac{1/k}{1-(\omega/\omega_n)^2 + 2\zeta(\alpha/\omega_n) + (\alpha/\omega_n)^2 + \mathrm{j}2(\zeta+\alpha/\omega_n)\omega/\omega_n}. \tag{9}$$

Eq. (9) shows that the exponential-windowed FRF is still different from the theoretical FRF given in Eq. (5), although the effect of its decay rate in the imaginary part of the denominator of Eq. (9) can be removed by modal analysis technique.

2.3. Expression of finite record length error for multi-dof system

The equation of motion of the viscously damped n-dof system is described as follows

$$[M]\{\ddot{x}(t)\} + [C]\{\dot{x}(t)\} + [K]\{x(t)\} = \{f(t)\}. \tag{10}$$

A FRF of Eq. (10), the displacement response of a point l by the exciting force of a point i, is theoretically known as

$$H_{il}(\omega) = \frac{X_l(\omega)}{F_i(\omega)} = \sum_{r=1}^{n} \frac{\phi_{lr}\phi_{ir}}{(k_r - \omega^2 m_r + \mathrm{j}\omega c_r)}, \tag{11}$$

where $F_i(\omega)$, $X_l(\omega)$, ϕ_{ir} and ϕ_{lr} are the spectrum of the force input, the spectrum of the displacement output, the value of the rth natural modal vectors of a point i and the value of a point l, respectively. And k_r, m_r and c_r represent respectively the modal stiffness, mass, and damping coefficient of the multi-dof system given in Eq. (10).

On the other hand, if the exciting force of the Dirac delta function is applied to a point i, the unit impulse response function at a point l will be [11–13]

$$h_{il}(t) = \sum_{r=1}^{n} \frac{\phi_{lr}\phi_{ir}}{m_r \omega_{dr}} \mathrm{e}^{-\zeta_r \omega_{nr} t} \sin \omega_{dr} t. \tag{12}$$

Since the signal should be acquired for only a record length T_{RL} in a real situation, the Fourier transformation of the unit impulse response given in Eq. (12) can be calculated as

$$\bar{H}_{il}(\omega)|_{T_{\mathrm{RL}}>0} = \int_{-0}^{T_{\mathrm{RL}}} h_{il}(t)\mathrm{e}^{-\mathrm{j}\omega t}\mathrm{d}t = \sum_{r=1}^{n} \frac{\phi_{lr}\phi_{ir}}{k_r - \omega^2 m_r + \mathrm{j}\omega c_r}[1 - E_r(\mathrm{j}\omega)|_{T_{\mathrm{RL}}}], \tag{13}$$

where

$$E_r(\omega)|_{T_{\mathrm{RL}}} = \mathrm{e}^{-(\zeta\omega_{nr}+\mathrm{j}\omega)T_{\mathrm{RL}}} \left\{ \frac{\zeta_r}{\sqrt{1-\zeta_r^2}} \sin \omega_{dr} T_{\mathrm{RL}} + \cos \omega_{dr} T_{\mathrm{RL}} + \mathrm{j}\frac{\omega}{\omega_{dr}} \sin \omega_{dr} T_{\mathrm{RL}} \right\}. \tag{14}$$

In this paper, $E_r(\omega)\big|T_{\mathrm{RL}}$ in Eq. (14) is called as the finite record length error of the rth mode of the FRF. As mentioned at the previous paragraph, Eq. (13) shows that the exact FRF of a multi-dof system cannot be also obtained from the impulse response spectrum as long as the record length T_{RL} is finite.

Until now, the unit impulse response function has been analytically dealt with to show the existence and characteristics of the finite record length error. The finite record length error should be properly dealt with in discrete data to usefully remove this error in an actual impact hammer testing. From now on, the spectrum of discrete signals of an impulse force and its impulse response is considered to improve the FRF obtained by an impact hammer testing. Although there may be different expressions, in dynamic signal analyzer the impulse response spectrum is

actually obtained from the following equation:

$$\hat{H}_{il}(k\Delta f) = \frac{X_l(k\Delta f)}{F_i(k\Delta f)}, \quad k = 0, 1, \ldots, N/2. \tag{15}$$

In Eq. (15), the denominator which is the discrete Fourier transformation of an impulsive force may have no finite record length error because the signal of impact force is certainly much shorter than the record length in any impact hammer testing. But the numerator of Eq. (15), the discrete Fourier transformation of the impulse response has the finite record length error when the record length is not sufficiently long. Consequently, the FRF obtained from the impact hammer testing cannot avoid the finite record length error in case that the record length is not longer than the duration time for complete disappearance of the impulse response. The record length should be properly chosen according to the signal processing ability of the dynamic analyzer, frequency resolution, the ratio of signal to noise (S/N ratio) and so on. Since the duration time of a lightly damped structure is too long to completely acquire all the signals, it is necessary to improve the impulse response spectrum in order to get a better FRF.

3. Improvement of impulse response spectrum

In this section, the correct expression of the impulse response spectrum including the finite record length error is theoretically derived, and an optimization method is introduced to reduce the error and get more improved FRF of the system.

3.1. Impulse response spectrum entailing finite record length error

As shown in Eq. (2), the unit impulse response function of a multi-dof system can be expressed as

$$h(t) = \sum_{r=1}^{n} A_r \mathrm{e}^{-\sigma_r t} \sin \omega_{dr} t, \tag{16}$$

$$A_r = \frac{\phi_{lr}\phi_{ir}}{m_r \omega_{dr}}, \tag{16a}$$

$$\sigma_r = \zeta_r \omega_{nr}, \tag{16b}$$

$$\omega_{dr} = \sqrt{1 - \zeta_r^2}\,\omega_{nr}. \tag{16c}$$

In Eq. (16), A_r, σ_r, and ω_{dr} are the rth modal constant, the rth modal damping and the rth damped angular frequency of the system, respectively. If the signal of Eq. (16) is digitized with a sampling time Δt and a discrete Fourier transformation applied, then the impulse response spectrum can be written as

$$\tilde{H}(k\Delta f) = \frac{T_{\mathrm{RL}}}{N} \sum_{i=0}^{N-1} \sum_{r=1}^{n} A_r \mathrm{e}^{-\sigma_r i T_{\mathrm{RL}}/N} \sin[\omega_{dr} i \Delta t] \mathrm{e}^{-\mathrm{j}2\pi k i/N}, \quad k = -\frac{N}{2}, \ldots, \frac{N}{2} - 1, \tag{17}$$

where N represents the number of data for discrete Fourier transformation, and n is the degree of freedom of the system. Using the sum's formula of geometric progression, Eq. (17) can be rewritten as

$$\tilde{H}(k\Delta f) = \frac{T_{\mathrm{RL}}}{2j}\sum_{r=1}^{n} A_r\left[\frac{1-\mathrm{e}^{-[\sigma_r T_{\mathrm{RL}}-\mathrm{j}2\pi(a_r-k)]}}{N[1-\mathrm{e}^{-[\sigma_r T_{\mathrm{RL}}-\mathrm{j}2\pi(a_r-k)]/N}]} - \frac{1-\mathrm{e}^{-[\sigma_r T_{\mathrm{RL}}+\mathrm{j}2\pi(a_r+k)]}}{N[1-\mathrm{e}^{-[\sigma_r T_{\mathrm{RL}}+\mathrm{j}2\pi(a_r+k)]/N}]}\right],$$
$$k = -\frac{N}{2},\ldots,-1,0,1,\ldots,\frac{N}{2}-1, \tag{18}$$

where

$$a_r = \frac{f_{dr}}{\Delta f} = f_{dr}T_{\mathrm{RL}} = \frac{\omega_d}{2\pi}T_{RL} \tag{19}$$

means the number of sinusoidal waves of rth mode which exists within the record length T_{RL}. Since a_r generally is a real number, it should be divided into an integer part and a decimal fraction part as follows:

$$a_r = p_r\ (\text{integer part}) + q_r\ (\text{decimal fraction part}) \tag{20}$$

where the integer number p_r stands for a serial number pointing out the peak of the rth mode on the impulse response spectrum, and the decimal fraction number q_r describes the resolution error which disturbs to find the exact peak frequency on the spectrum. Assuming the number of data N in Eq. (18) to be sufficiently large and substituting Eq. (20) into Eq. (18), the impulse response spectrum is rewritten as

$$\tilde{H}(k\Delta f) = \frac{T_{\mathrm{RL}}}{2}\sum_{r=1}^{n} A_r\left[\frac{1-\mathrm{e}^{-\sigma_r T_{\mathrm{RL}}}\mathrm{e}^{\mathrm{j}2\pi\{(p_r+q_r)-k\}}}{2\pi\{(p_r+q_r)-k\}+\mathrm{j}\sigma_r T_{\mathrm{RL}}} + \frac{1-\mathrm{e}^{-\sigma_r T_{\mathrm{RL}}}\mathrm{e}^{-\mathrm{j}2\pi\{(p_r+q_r)+k\}}}{2\pi\{(p_r+q_r)+k\}-\mathrm{j}\sigma_r T_{\mathrm{RL}}}\right]. \tag{21}$$

Eq. (21) is the expression of the unit impulse response spectrum including the finite record length error.

When the impulse response spectrum $\hat{H}_{il}(k\Delta f)$ of Eq. (15) obtained by an impact hammer testing is compared to $\tilde{H}(k\Delta f)$ of Eq. (21) derived from the unit impulse response function, their magnitude and phase should be exactly the same at all frequencies.

There are results available for a single dof method by which the unknown parameters A_r, σ_{r}, and q_r in Eq. (21) can be directly calculated from the correct expression of a single dof FRF including the finite record length errors [7,8]. In this method, the rth modal damping σ_{r} of each mode is firstly calculated by solving the following equation:

$$\sigma_r = \frac{\pi}{T_{\mathrm{RL}}}\sqrt{-\left(\frac{R_{r+}^2-R_{r-}^2}{R_{r+}^2+R_{r-}^2-2}\right)^2 + \frac{8}{R_{r+}^2+R_{r-}^2-2}}, \tag{22}$$

where R_{r+} and R_{r-} represent the ratio of the rth peak value to the fore and aft values of the peak respectively. The previous research also derived the following equations which show the relation

of the unknown parameters:

$$R_{r-}^2 = \left|\frac{\hat{H}[p_r\Delta f]}{\hat{H}[(p_r-1)\Delta f]}\right|^2 = \frac{[2p_r(q_r+1)+(\sigma_r T_{\mathrm{RL}}/2\pi)^2]^2+[2(\sigma_r T_{\mathrm{RL}}/2\pi)]^2}{[q_r\cdot 2p_r+(\sigma_r T_{\mathrm{RL}}/2\pi)^2]^2+[2(\sigma_r T_{\mathrm{RL}}/2\pi)p_r]^2}, \tag{23}$$

$$R_{r+}^2 = \left|\frac{\hat{H}[p_r\Delta f]}{\hat{H}[(p_r+1)\Delta f]}\right|^2 = \frac{[2p_r(q_r-1)+(\sigma_r T_{\mathrm{RL}}/2\pi)^2]^2+[2(\sigma_r T_{\mathrm{RL}}/2\pi)]^2}{[q_r\cdot 2p_r+(\sigma_r T_{\mathrm{RL}}/2\pi)^2]^2+[2(\sigma_r T_{\mathrm{RL}}/2\pi)p_r]^2}, \tag{24}$$

where $\hat{H}[p_r\Delta f]$ is the peak value showing on the spectrum obtained by impact hammer testing, and $\hat{H}[(p_r-1)\Delta f]$ and $\hat{H}[(p_r+1)\Delta f]$ are the fore and aft values of the peak, respectively. By using the above Eqs. (19)–(24), the unknown parameters of each mode of the FRF can be directly calculated [7,8]. The parameters calculated by the single dof method cannot avoid some errors caused by mode coupling of the multi-dof system because of the assumption of the single dof model. Nevertheless, this single dof method is still useful for a lightly damped model, to find initial values of an optimization method which will be introduced below.

3.2. FRF of multi-dof model improved by an optimization algorithm

Each mode of the multi-dof system is actually coupled with its adjacent modes so that mode coupling should be considered to estimate more accurate FRF from an impulse response spectrum. In this paper, an optimization algorithm is applied to the impulse response spectrum entailing the finite record length error in order to calculate the unknown parameters of the impulse response function, such as the rth modal constant value A_r, the rth modal damping σ_r and the rth damped natural frequency ω_{dr} in Eq. (16).

The ultimate purpose of the optimization method proposed in this paper is to minimize the discrepancies between the impulse response spectrum obtained by the experiments given in Eq. (15) and the expression of the spectrum entailing the finite record length error given in Eq. (21). In order to establish the cost function of the optimization algorithm, first of all, the right-hand side of Eq. (21) is divided into a real part and an imaginary part as follows [8]

$$\tilde{H}(k\Delta f) = \mathrm{Re}[\tilde{H}(k\Delta f)] + \mathrm{j}\,\mathrm{Im}[\tilde{H}(k\Delta f)], \tag{25}$$

where

$$\begin{aligned}\mathrm{Re}[\tilde{H}(k\Delta f)] = T_{\mathrm{RL}}\sum_{r=1}^{n} A_r \mathrm{e}^{-\sigma_r T_{\mathrm{RL}}}[&-16\pi^2 T_{\mathrm{RL}} k^2\sigma_r \sin 2\pi q_r + \{4\pi^2((p_r+q_r)^2-k^2)+T_{\mathrm{RL}}^2\sigma_r^2\}\\ &\times\{4\pi(p_r+q_r)(\mathrm{e}^{\sigma_r T_{\mathrm{RL}}}-\cos 2\pi q_r) - 2T_{\mathrm{RL}}\sigma_r \sin 2\pi q_r\}]\\ &\div[16\pi^2 T_{\mathrm{RL}}^2 k^2\sigma_r^2 + \{4\pi^2((p_r+q_r)^2-k^2)+T_{\mathrm{RL}}^2\sigma_r^2\}^2],\end{aligned}$$

$$\begin{aligned}\mathrm{Im}[\tilde{H}(k\Delta f)] = -T_{\mathrm{RL}}\sum_{r=1}^{n} A_r 4\pi k \mathrm{e}^{-\sigma_r T_{\mathrm{RL}}}&[4\pi(p_r+q_r)T_{\mathrm{RL}}\sigma_r(\mathrm{e}^{\sigma_r T_{\mathrm{RL}}}-\cos 2\pi q_r)\\ &+\{4p_r^2\pi^2+8p_r q_r\pi^2+4\pi^2(q_r^2-k^2)+T_{\mathrm{RL}}^2\sigma_r^2\}\sin 2\pi q_r]\\ &\div[16\pi^2 T_{\mathrm{RL}}^2 k^2\sigma_r^2 + \{4\pi^2((p_r+q_r)^2-k^2)+T_{\mathrm{RL}}^2\sigma_r^2\}^2].\end{aligned}$$

Eq. (25), a function including the parameters q_r, A_r and σ_r, can be simply expressed as follows

$$\tilde{H}_k(\{q\}^{\mathrm{T}},\{A\}^{\mathrm{T}},\{\sigma\}^{\mathrm{T}}) = \tilde{H}_{Rk}(\{q\}^{\mathrm{T}},\{A\}^{\mathrm{T}},\{\sigma\}^{\mathrm{T}}) + \mathrm{j}\tilde{H}_{Ik}(\{q\}^{\mathrm{T}},\{A\}^{\mathrm{T}},\{\sigma\}^{\mathrm{T}}), \tag{26}$$

where

$$\tilde{H}(\{q\}^{\mathrm{T}},\{A\}^{\mathrm{T}},\{\sigma\}^{\mathrm{T}}) = \tilde{H}(q_1,\ldots,q_n,A_1,\ldots,A_n,\sigma_1,\ldots,\sigma_n).$$

In Eq. (26), $\tilde{H}_k(\{q\}_{,}^{\mathrm{T}}\{A\}_{,}^{\mathrm{T}}\{\sigma\}^{\mathrm{T}})$, a complex value of the impulse response spectrum entailing the finite record length error, is divided into the real part $\tilde{H}_{Rk}(\{q\}_{,}^{\mathrm{T}}\{A\}_{,}^{\mathrm{T}}\{\sigma\}^{\mathrm{T}})$ and the imaginary part $\tilde{H}_{Ik}(\{q\}_{,}^{\mathrm{T}}\{A\}_{,}^{\mathrm{T}}\{\sigma\}^{\mathrm{T}})$. Now the differences of magnitude between the experimental spectrum of Eq. (15) and the correct expression of Eq. (25) are summed at all the frequencies. And the summed value is defined as a cost function for the optimization method which represents at the following equation:

$$\begin{aligned} J[\{q\}^{\mathrm{T}},\{A\}^{\mathrm{T}},\{\sigma\}^{\mathrm{T}}] = {} & \sum_{k=0}^{N/2-1} \{\tilde{H}_{Rk}(\{q\}^{\mathrm{T}},\{A\}^{\mathrm{T}},\{\sigma\}^{\mathrm{T}}) - \mathrm{Re}[\hat{H}(k\Delta f)]\}^2 \\ & + \sum_{k=0}^{N/2-1} \{\tilde{H}_{Ik}(\{q\}^{\mathrm{T}},\{A\}^{\mathrm{T}},\{\sigma\}^{\mathrm{T}}) - \mathrm{Im}[\hat{H}(k\Delta f)]\}^2, \end{aligned} \tag{27}$$

where $\hat{H}(k\Delta f)$ is a complex value of the impulse response spectrum obtained by an impact hammer testing at a frequency $k\Delta f$. In Eq. (27), the $3n$ values of the frequency errors q_r, the modal constant values A_r, and the modal dampings $\sigma_r\,(r=1,\ldots,n)$ are regarded as the design parameters of the optimization. For convenience of mathematical expression, the $3n$ design parameters is represented as $u_i\,(i=1,\ldots,3n)$. If the cost function in Eq. (27) is differentiated over the design parameters to determine their optimum values minimizing the cost, the following equation is obtained:

$$\frac{\partial J}{\partial u_i} = 2\sum_{k=0}^{N/2-1}\left(\{\tilde{H}_{Rk} - \mathrm{Re}[\hat{H}(k\Delta f)]\}\frac{\partial \tilde{H}_{Rk}}{\partial u_i} + \{\tilde{H}_{Ik} - \mathrm{Im}[\hat{H}(k\Delta f)]\}\frac{\partial \tilde{H}_{Ik}}{\partial u_i}\right), \quad i=1,\ldots,3n. \tag{28}$$

According to the Gauss–Newton method [14], the search direction for optimum values is determined by solving the following simultaneous equation:

$$\sum_{j=1}^{3n}\frac{\partial^2 J}{\partial u_i\,\partial u_j}\Delta u_j = -\frac{\partial J}{\partial u_i}, \quad i=1,\ldots,3n. \tag{29}$$

In this paper, the second-order differentiations in Eq. (29) are approximated by the first-order differentiations as follows:

$$\frac{\partial^2 J}{\partial u_i\,\partial u_j} = 2\sum_{k=0}^{N/2-1}\left(\frac{\partial \tilde{H}_{Rk}}{\partial u_i}w_k\frac{\partial \tilde{H}_{Rk}}{\partial u_j} + \frac{\partial \tilde{H}_{Ik}}{\partial u_i}w_k\frac{\partial \tilde{H}_{Ik}}{\partial u_j}\right), \tag{30}$$

$$-\frac{\partial J}{\partial u_i} = 2\sum_{k=0}^{N/2-1}\left(\frac{\partial \tilde{H}_{Rk}}{\partial u_i}w_k(\mathrm{Re}[\hat{H}(k\Delta f)] - \tilde{H}_{Rk}) + \frac{\partial \tilde{H}_{Ik}}{\partial u_i}w_k(\mathrm{Im}[\hat{H}(k\Delta f)] - \tilde{H}_{Ik})\right), \tag{31}$$

where w_k is the weighting factor with respect to a frequency $k\Delta f$. Once the suitable direction for optimum design changes is calculated by Eqs. (29)–(31), the step size α can be determined by the golden section search method [14].

$$\{u\}^{(m+1)} = \{u\}^{(m)} + \alpha\{\Delta u\}. \tag{32}$$

New values of the design parameters calculated by Eq. (32) are used for the next step of the optimization method. This process is repeated until new design parameters $u_i\,(i = 1, \ldots, 3n)$, or q_r, A_r, $\sigma_r\,(r = 1, \ldots, n)$, make the cost function be a minimum. Once the optimum values of the parameters q_r, A_r, σ_r are estimated, the improved FRF is calculated by the following equation which is a revision of Eq. (11) composed of the design parameters:

$$H(\omega) = \sum_{r=1}^{n} \frac{2\pi\Delta f(p_r + q_r)A_r}{\{4\pi^2\Delta f^2(p_r + q_r)^2 + \sigma_r^2 - \omega^2 + \mathrm{j}2\sigma_r\omega\}}. \tag{33}$$

In Eq. (33), the serial number of rth mode peak p_r and the frequency resolution Δf are readable on the impulse response spectrum obtained by the impact hammer testing.

4. Numerical and experimental examples

4.1. Numerical example

The 3-dof lightly damped model shown in Fig. 1 is numerically simulated to show whether the finite record length error takes place in the impulse response spectrum according to the length of recording time. In this example, the response of the model is calculated by the Runge–Kutta method when the force $f(t)$ is impulsively enforced.

To show a case of almost no finite record length error, the impulse response is calculated with 16,348 (2^{14}) steps for 20 s. The impulsive force and the response signals obtained are plotted in Fig. 2. The frequency-magnitude and Nyquist plot of the impulse response spectrum are plotted in Figs. 3 and 4, respectively, which are compared with the exact FRF theoretically obtained by

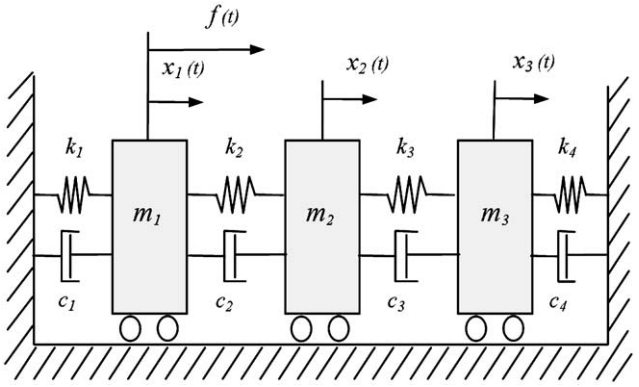

Fig. 1. A 3-dof damped model ($m_1 = m_2 = m_3 = 3\,\mathrm{kg}$, $k_1 = k_2 = k_3 = 15,000\,\mathrm{N/m}$, $c_1 = c_2 = c_3 = 0.2\,\mathrm{N/m/s}$).

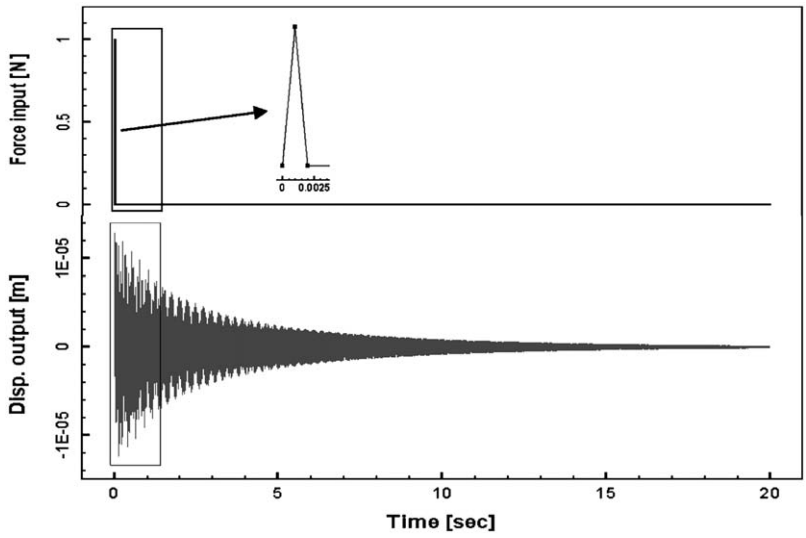

Fig. 2. Impulse force and its response signals for the model in Fig. 1 (16,348 samples for 20 s).

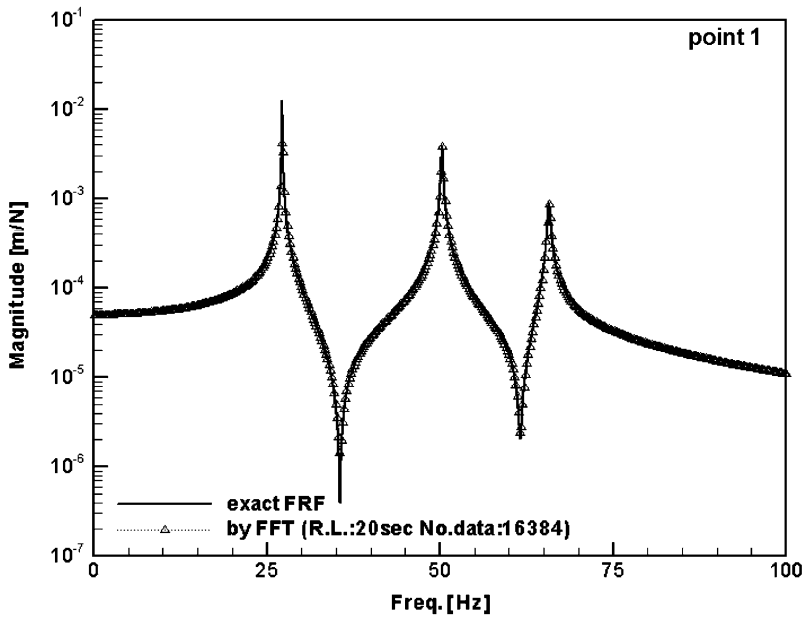

Fig. 3. Comparison between the theoretical FRF and the impulse response spectrum (in case of 16,348 samples for 20 s).

modal analysis [11,12]. It is shown from Figs. 3 and 4 that the impulse response spectrum is well matched to the exact FRF except the frequency resolution error when the record length is sufficiently long.

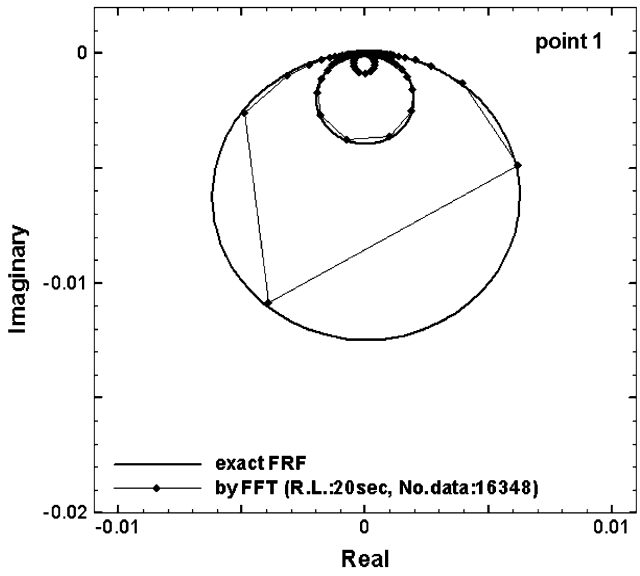

Fig. 4. Comparison between Nyquist plot of the theoretical FRF and one of the impulse response spectrum (in case of 16,348 samples for 20 s).

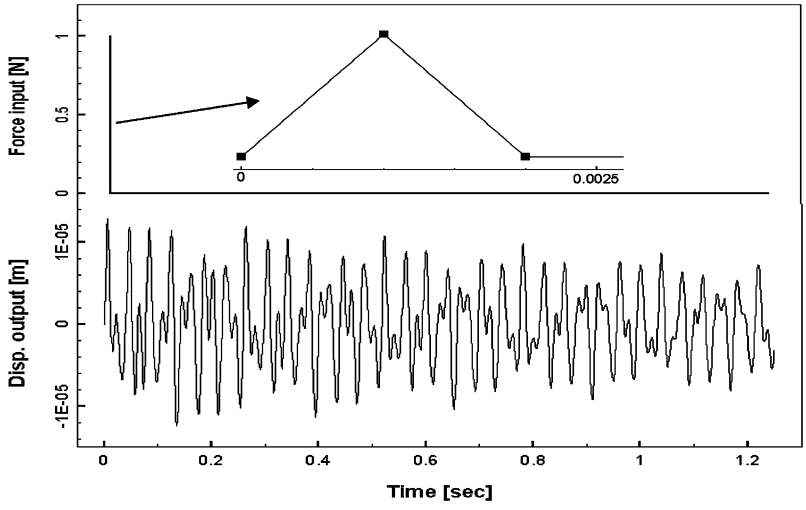

Fig. 5. Impulse force and its response signals for the model in Fig. 1 (1024 samples for 1.25 s).

It must be considered that the record length is limited by various reasons, such as capacity of memory resister, computation time, the ratio of signal to noise (S/N ratio) and so forth. The force and its response signal of 1024 data for 1.25 s are plotted in Fig. 5, which is referred as a insufficient record length. The frequency-magnitude and Nyquist plot of the impulse response spectrum are plotted in Figs. 6 and 7, respectively, and are compared with the exact FRF. It is

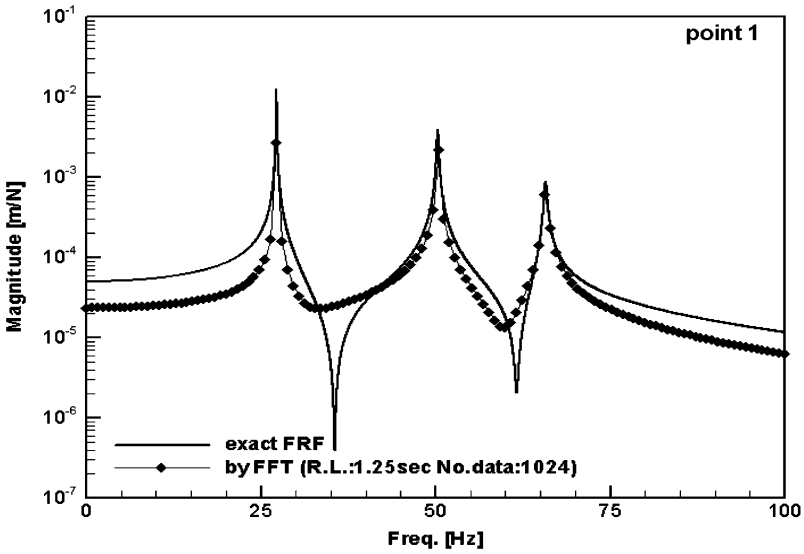

Fig. 6. Comparison between the theoretical FRF and the impulse response spectrum (in case of 1024 samples for 1.25 s).

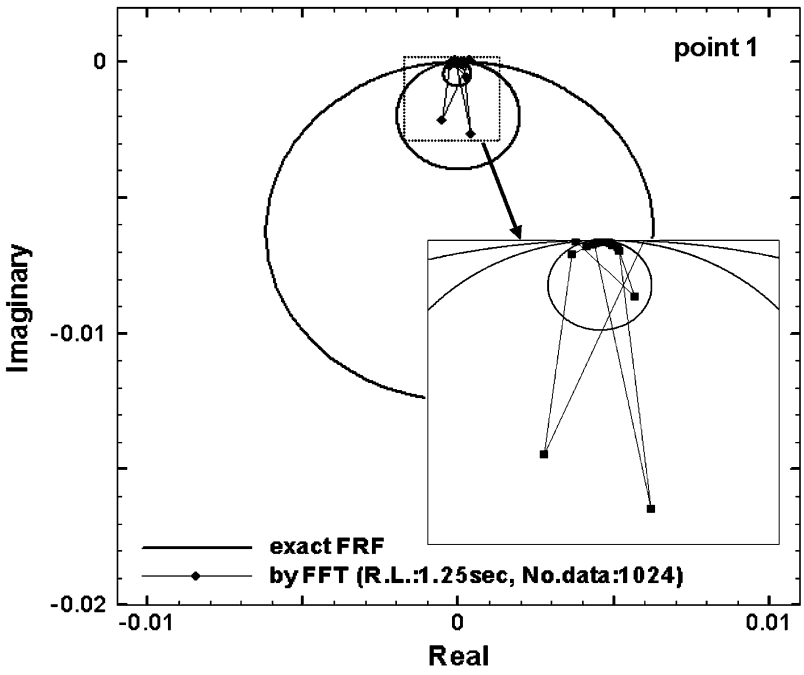

Fig. 7. Comparison between Nyquist plot of the theoretical FRF and one of the impulse response spectrum (in case of 1024 samples for 1.25 s).

Table 1
Initial and optimum values of the system parameters obtained by the single dof method and the optimization method, respectively

	Initial	Optimum	Exact
q_1	-0.0402	0.0477	0.0479
q_2	-0.1227	-0.0885	-0.0883
q_3	0.2565	0.1982	0.1988
A_1	4.95×10^{-3}	4.85×10^{-3}	4.87×10^{-3}
A_2	4.80×10^{-3}	5.21×10^{-3}	5.27×10^{-3}
A_3	1.63×10^{-3}	1.97×10^{-3}	2.02×10^{-3}
σ_1	0.230	0.195	0.195
σ_2	0.501	0.669	0.667
σ_3	0.674	1.131	1.138

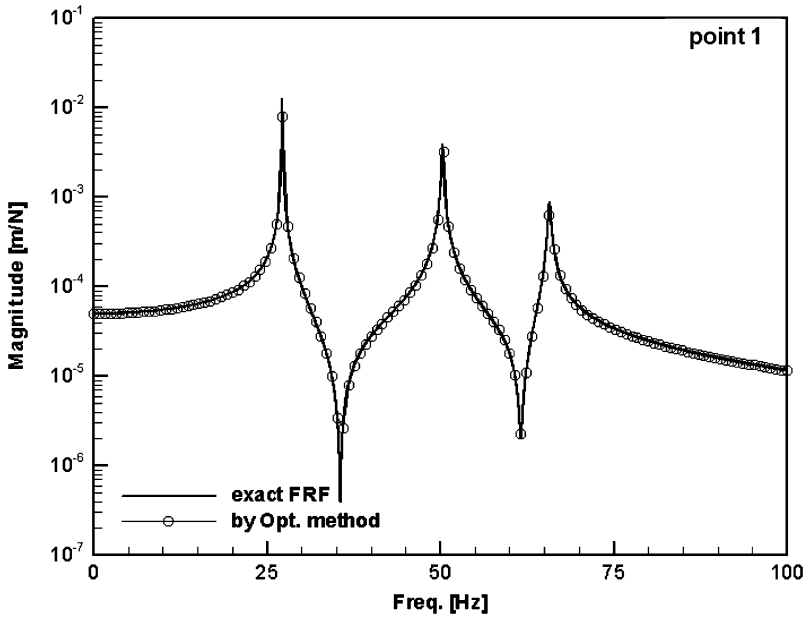

Fig. 8. Comparison between the theoretical FRF and the improved FRF by an optimization method.

shown from Figs. 6 and 7 that the impulse response spectrum is different from the exact FRF when the record length is not properly long.

In this simulation example, the optimization method is applied to the impulse response spectrum entailing the finite record length to show the validity of its results. To calculate the parameters q_r, A_r and σ_r as initial values of the optimization method, the single dof method is used. The initial and the optimum values are compared with the exact values in Table 1. The frequency-magnitude and Nyquist plot obtained by substituting the optimum values into Eq. (33)

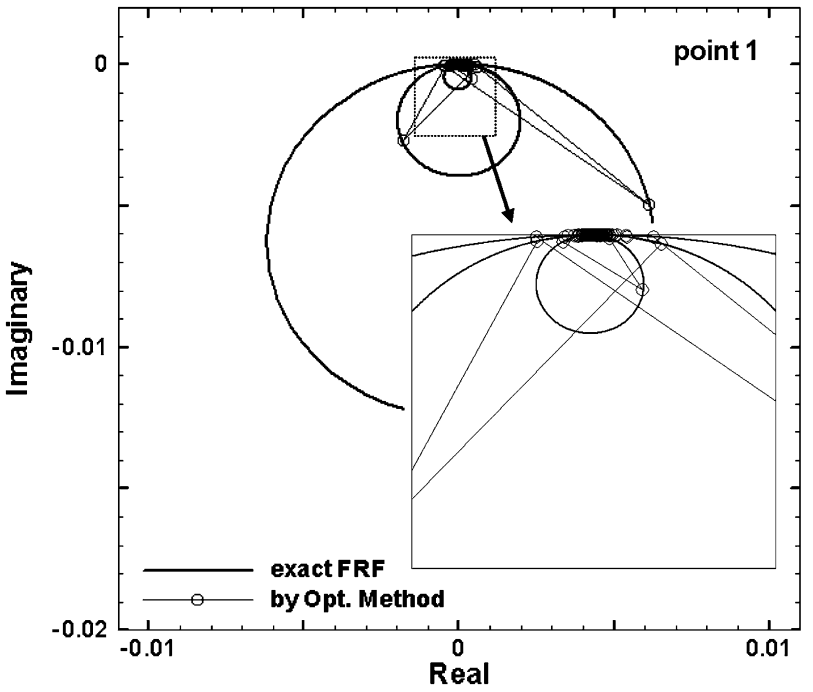

Fig. 9. Comparison between Nyquist plot of the theoretical FRF and one of an improved FRF calculated by the optimization method.

are presented in Figs. 8 and 9, respectively. It is shown from these figures that the optimization method proposed in this paper is needed to calculate the improved FRF from the impulse response spectrum including the finite record length error.

4.2. Experimental example

An aluminum plate mounted on 4 rubber posts is used for an impact hammer testing. The aluminum plate has the length of 500 mm, the width 510 mm, the thickness 5.9 mm and the density 2193 kg/m^3. A plastic tip is mounted on the head of the impact hammer used in this experiment in order that the aluminum plate is excited up to the interesting frequency, 150 Hz, without significant error caused by the shape of the impulse signal. The time history is displayed in Fig. 10 when the plate is excited by an impact hammer. The vibration signal still oscillates after 8 s, which means that a record length longer than 8 s is necessary to get the correct FRF of the plate without the finite record length error. In Figs. 11 and 12, the magnitudes and phases of the impulse response spectrum using the record lengths of 8 s and 1 s are compared with those of the FRF improved by the optimization method with an impulse response spectrum of 1.0 s. In this paper, it is assumed that the impulse response spectrum of 8 s record length is nearly close to the exact FRF of the rubber-mounted plate because its record length is sufficiently long for the acceleration response to disappear. It is clear from Figs. 11 and 12 that the impulse response spectrum of 1 s record length is different from that of 8 s in the magnitude and phase because of its finite record

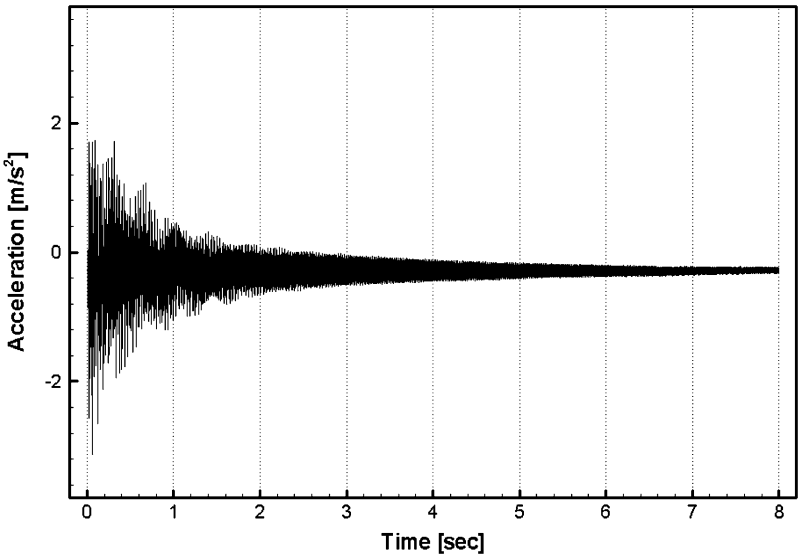

Fig. 10. Acceleration signal of an impulse response for a plate.

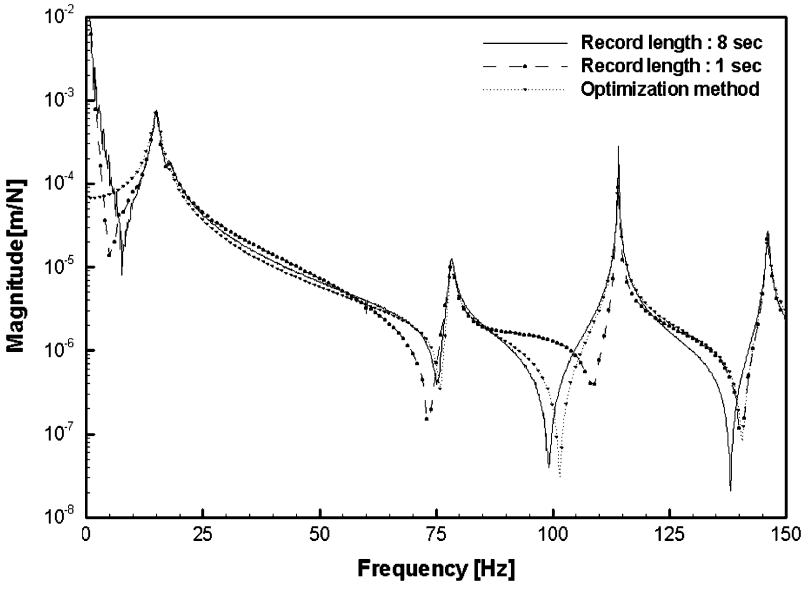

Fig. 11. Magnitudes of two impulse response spectra with 1.0 s record length, 8.0 s record length, and the improved FRF.

length error. On the other hand, the improved FRF estimated by the proposed method matches well with the exact FRF in both magnitude and phase if it is assumed that 180 and -180° phase are the same as in Fig. 12.

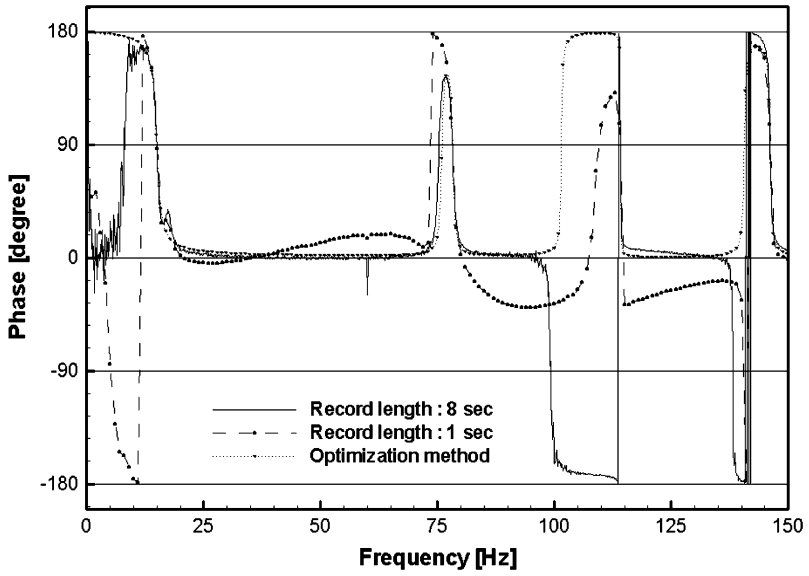

Fig. 12. Phases of two impulse response spectrums with 1.0 s record length, 8.0 s record length, and the improved FRF.

5. Conclusion

This paper dealt with a special error which occurs in impact hammer testing, especially when record length is not sufficiently long. This kind of error, called as a finite record length error, is uncovered, formulated by the theoretical process, and improved by the single dof method and the optimization method. Some examples are carried out to show both the characteristics of the finite record length error and the effect of the optimization method. The conclusion of this paper can be summarized as the following:

(1) The finite record length error, which makes the impulse response spectrum to be different from the exact FRF, is theoretically formulated.
(2) Exponential window used to reduce some errors including the finite record length error causes a bias error of the impulse response spectrum.
(3) The single dof method directly estimating the system parameters from an impulse response spectrum including the finite record length error is applied to a multi-dof system and an optimization method is proposed to improve the accuracy of the parameters.
(4) Numerical and experimental examples showed the effectiveness of the proposed method to reduce the finite record length error.

Acknowledgements

The authors would like to thank the Ministry of Science and Technology of Korea for the financial support by a Grant (M1-0203-00-0017) under the NRL (National Research Laboratory).

This work was supported by the Post-doctoral Fellowship Program of Korea Science & Engineering Foundation (KOSEF).

References

[1] P.K. Roy, N. Ganesan, Transient response of a cantilever beam subjected to an impulse load, *Journal of Sound and Vibration* 183 (5) (1995) 873–890.
[2] A.J. Stanley, N. Ganesan, Impulse response of cylindrical shells with a discontinuity in the thickness subjected to an axisymmetric load, *Journal of Sound and Vibration* 184 (3) (1995) 369–387.
[3] D.J. Ewins, *Modal Testing: Theory and Practice*, Research Studies Press, Baldock, UK, 1986.
[4] H. Dishan, Phase error in fast Fourier transform analysis, *Mechanical Systems and Signal Processing* 9 (2) (1995) 113–118.
[5] W. Fladung, R. Rost, Application and correction of the exponential window for frequency response function, *Mechanical Systems and Signal Processing* 11 (1) (1997) 23–36.
[6] J.C. Burgess, On digital spectrum analysis of periodic signals, *Journal of the Acoustical Society of America* 58 (3) (1975) 556–567.
[7] W.B. Jeong, S.J. Ahn, H.Y. Chang, C.H. Chang, The improvement of leakage error in digital Fourier transform, *The Korean Society for Noise and Vibration Engineering* 11 (3) (2001) 455–460.
[8] S.J. Ahn, W.B. Jeong, The errors and reducing method in 1-d.o.f. frequency response function from impact hammer testing, *The Korean Society for Noise and Vibration Engineering* 12 (9) (2002) 702–708.
[9] S.J. Ahn, W.B. Jeong, W.S. Yoo, Unbiased expression of FRF with exponential-window function in impact hammer testing, *Journal of Sound and Vibration* 277 (4–5) (2004) 931–941.
[10] S.J. Ahn, W.B. Jeong, The improvement of muti-d.o.f. impulse response spectrum by using optimization technique, *The Korean Society for Noise and Vibration Engineering* 12 (10) (2002) 792–798.
[11] A. Nagamatsu, *Modal Analysis*, Baifukan, Japan, 1985.
[12] N.M.M. Maia, J.M.M. Silva, *Theoretical and Experimental Modal Analysis*, Research Studies Press, London, 1998.
[13] J.S. Bendat, A.G. Piersol, *Random Data: Analysis and Measurement Procedures*, Wiley, New York, 1986.
[14] S. Arora, *Introduction to Optimum Design*, McGraw-Hill, New York, 1989.